Article

Enzymatic SPR Approach for the Detection of Nano and Microplastic Particles Using Rainwater as Matrices

Denise Margarita Rivera-Rivera [1,2], Gabriela Elizabeth Quintanilla-Villanueva [3], Donato Luna-Moreno [3], Jonathan Muthuswamy Ponniah [4], José Manuel Rodríguez-Delgado [5], Erika Iveth Cedillo-González [6,7], Garima Kaushik [8], Juan Francisco Villarreal-Chiu [1,2,*] and Melissa Marlene Rodríguez-Delgado [1,2,*]

1 Universidad Autónoma de Nuevo León, Facultad de Ciencias Químicas, Av. Universidad S/N Ciudad Universitaria, San Nicolás de los Garza 66455, Mexico; denise.rivera@unicepes.edu.mx
2 Centro de Investigación en Biotecnología y Nanotecnología (CIByN), Facultad de Ciencias Químicas, Universidad Autónoma de Nuevo León, Parque de Investigación e Innovación Tecnológica, Km. 10 Autopista al Aeropuerto Internacional Mariano Escobedo, Apodaca 66629, Mexico
3 Centro de Investigaciones en Óptica AC, Div. de Fotónica, Loma del Bosque 115, Lomas del Campestre, León 37150, Mexico; quintanillagabriela@cio.mx (G.E.Q.-V.); dluna@cio.mx (D.L.-M.)
4 Centro Interdisciplinario de Investigaciones y Estudios Sobre Medio Ambiente y Desarrollo, Instituto Politécnico Nacional (CIIEMAD-IPN), Calle 30 de Junio 1520, Gustavo A. Madero, Ciudad de Mexico 07340, Mexico; jmuthuswamy@ipn.mx
5 Tecnológico de Monterrey, School of Engineering and Sciences, Av. Eugenio Garza Sada Sur 2501, Col. Tecnológico, Monterrey 64849, Mexico; jmrd@tec.mx
6 Department of Engineering "Enzo Ferrari", University of Modena and Reggio Emilia, Via Vivarelli 10/1, 41125 Modena, Italy; ecedillo@unimore.it or erika.cedillo@pelucco.com
7 Pelucco R&D Division, Lombardia, Av. Primavera, Apodaca 66612, Mexico
8 Department of Environmental Science, School of Earth Sciences, Central University of Rajasthan, Ajmer 305817, Rajasthan, India; garimakaushik@curaj.ac.in
* Correspondence: juan.villarrealch@uanl.edu.mx (J.F.V.-C.); melissa.rodriguezdl@uanl.edu.mx (M.M.R.-D.)

Abstract

The increasing presence of microplastics (MPs) and nanoplastics (NPs) in environmental matrices presents substantial analytical challenges due to their small size and chemical diversity. This study introduces a novel enzymatic biosensor based on the Surface Plasmon Resonance (SPR) platform for the sensitive detection of MPs and NPs, utilizing laccase as the recognition element. Standard plastic particles, including polystyrene (PS, 0.1 µm), polymethyl methacrylate (PMMA, 1.0 µm and 100 µm), and polyethylene (PE, 34–50 µm), were analyzed using SPR angular interrogation along with a fixed-angle scheme. The angular approach revealed a clear relationship between the resonance angle, particle size, and refractive index, while the fixed-angle method, combined with immobilized laccase, facilitated specific detection through enzyme/substrate interactions. The analytical parameters showed detection limits ranging from 7.5×10^{-4} µg/mL (PE, 34–50 µm) to 253.2 µg/mL (PMMA, 1 µm), with significant differences based on polymer type and enzymatic affinity. Application of the biosensor to real rainwater samples collected from two regions in Mexico (Tula and Molango) confirmed its functionality, although performance varied depending on matrix composition, exhibiting inhibition in samples with high manganese (Mn^{2+}), chromium (Cr^{2+}), and zinc (Zn^{2+}) content. Despite these limitations, the sensor achieved a 113% recovery rate in Tula rainwater, demonstrating its potential for straightforward in situ environmental monitoring. This study highlights the capabilities of laccase-based SPR biosensors in enhancing microplastic detection and underscores the necessity of considering matrix effects for real-world applications.

Keywords: microplastics; nanoplastics; SPR biosensor; enzyme; laccase; rainwater

1. Introduction

The growing concern about microplastics (MPs) and nanoplastics (NPs) arises from their widespread accumulation, poor waste management, and global dispersal, which pose significant risks to ecosystems and human health [1]. Plastics are everywhere in modern life, with global production reaching 400 million tons in 2022 and expected to rise to 34 billion tons by 2050 [2]. When exposed to the environment, plastics fragment into smaller particles. MPs are defined as fragments smaller than 5 mm, while NPs range from 1 nm to 1 μm in size [3–5]. Due to their small size, these particles are easily spread in air, water, and soil, and can be ingested or absorbed by organisms, raising concerns about bioaccumulation and toxicity [6–8]. Accurately detecting and monitoring MPs and NPs in environmental matrices remains a significant challenge. Traditional techniques include scanning electron microscopy (SEM), which provides morphological characterization but is labor-intensive and unreliable for nanoscale particles [9,10]. Vibrational spectroscopy methods, such as Raman and Fourier-transform infrared spectroscopy (FTIR), are non-destructive and enable polymer identification through unique spectral fingerprints, although they are time-consuming and require point-by-point analysis [11,12]. Thermal techniques like pyrolysis-gas chromatography-mass spectrometry (py-GC-MS) and thermogravimetry (TGA) offer rapid and specific results, but they are destructive, require extensive preprocessing, and lack the ability to determine particle size and shape [13–15]. Most of these methods demand specialized equipment and expertise, and they lack the molecular specificity provided by biological receptors.

Biosensors have emerged as promising alternatives, offering specificity, lower detection limits, and the potential for real-time monitoring in complex matrices. These systems incorporate biorecognition elements, such as enzymes, antibodies, or cells, coupled with a transducer that converts biochemical interactions into measurable signals (optical, electrochemical, or thermal) [16]. Several biosensors targeting MPs and NPs have been developed using different sensing mechanisms. For instance, Wang et al. (2022) designed an electrochemical biosensor using a carbon working electrode and electroactive bacteria as the recognition element [17]. The bacteria's current response decreased when interacting with MPs, indicating particle binding to the microbial biofilm [17]. Later, Gongi et al. (2022) developed an impedimetric sensor using cyanobacterial extracellular polymer as a sensing membrane, achieving detection of MPs from 0.1 μm to 1 mm [18]. The sensor measured the impedance shift of the MPs as they moved through the medium, showing a detection limit of 10 to 11 M [18]. Optical biosensing platforms, especially Surface Plasmon Resonance (SPR), offer label-free and real-time detection capabilities. In SPR systems, a metal film excites surface electrons when illuminated at a specific angle, and binding events on the surface alter the refractive index, leading to measurable shifts in reflected light intensity [19,20]. Huang et al. (2021) employed SPR chips functionalized with estrogen receptors to detect MPs (20 μm) in phosphate-buffered saline (PBS) [21]. The system distinguished plastic types based on binding affinity: polystyrene (PS, 0.05 nM) > polyvinyl chloride (PVC, 0.09 nM) > polyethylene (PE, 0.14 nM), measuring the refractive index variations in its interaction with the receptors [21].

Similarly, Seggio et al. (2024) used estrogen receptors on a gold nanograting platform to detect poly(methyl methacrylate) (PMMA) nanoparticles in seawater, achieving a detection limit of 0.39 ng/mL [22]. Another example of the use of SPR systems was reported by Oh et al. (2021), who developed a localized surface plasmon resonance (LSPR)-based gold nanoparticles (Au-NPs) system with bio-mimicked peptide targeting polystyrene nanoplastics through oligopeptide recognition [23]. Among bioreceptors, laccase enzymes have gained attention for their potential role in plastic recognition and degradation. These multicopper oxidases, naturally involved in lignin degradation, can catalyze oxidative

reactions on a wide range of substrates, including synthetic polymers; for example, laccase excreted by the actinomycete *Rhodococcus ruber* [24], *Trichoderma harzianum* [25], and the fungus *Aspergillus flavus* [26] have been reported in the biodegradation of polyethylene microplastics. The laccase enzymes oxidize the polymer, transforming it into carboxylic acids, which feature carbonyl groups (-C=O-) and ether groups that can be metabolized through β-oxidation and the Krebs cycle [26]. Similarly, laccase from *Cochliobolus* and *Pleurotus ostreatus* have been implicated in the biodegradation of polyvinyl chloride (PVC) [27] and polystyrene biodegradation [28,29]. The studies report that the catalytic activity of microplastics by laccases is based on oxidative reactions, similar to the degradation of lignin in nature [30]. The latest reports suggest that the binding of polymeric chains to the enzyme's active site generates certain groups on the polymer chains to oxidize, leading to the breakdown of C-C, C-O, and C-N linkages in particular, and generating the concomitant reduction of molecular oxygen to water due to the electron transfer occurring during the oxidation [31]. Furthermore, laccase has been reported to hydrolyze ester bonds in polyethylene terephthalate (PET) [32], expanding its potential as a plastic recognition element for biosensing applications, as there are no published reports on this use.

In this context, the present study aims to develop a biosensor platform using SPR technology integrated with laccase enzymes as biorecognition elements for the detection of micro- and nanoplastics. Standard particles of various sizes (100 μm, 34–50 μm, 1.0 μm, and 0.1 μm) were tested at different concentrations to assess the sensor's performance in controlled buffer solutions and complex matrices such as rainwater. The results seek to validate the platform's sensitivity, reproducibility, and real-world applicability. This research contributes to the ongoing effort to develop receptor-based detection systems with high affinity and specificity toward different types of plastics, enabling more reliable and accessible monitoring of microplastic contamination in environmental settings.

2. Materials and Methods

2.1. Reagents

Standard solutions of spherical polystyrene (PS diameter 0.1 μm), polymethyl methacrylate (PMMA, diameter 1.0 μm and 100 μm), and polyethylene (PE, diameter 34–50 μm) were purchased from Sigma-Aldrich (St. Louis, MO, USA) as aqueous suspensions at 10% w/v (10 mg/100 mL). From these suspensions, stock solutions at different concentrations were prepared in ultrapure water, and subsequently, working solutions were prepared by serial dilution in a water/phosphate-buffered saline solution (90:10, % v/v), pH 7.3. Laccase from *Rhus vernicifera* and the chemical compounds employed in its immobilization, N-hydroxysuccinimide (NHS), N-(3-dimethylaminopropyl)-N′-ethylcarbodiimide hydrochloride (EDC), ethanolamine, phosphate buffer saline 10 mM, pH 7.3 (PBS), 2-(N-morpholino)ethanesulfonic acid (MES), were obtained from Sigma-Aldrich (St. Louis, MO, USA).

2.2. Preparation of Microplastic Working Solution

Microplastic working solutions were prepared by serially diluting the stock particle suspension, covering concentrations from 0 to 9000 μg mL^{-1}. Additionally, real rainwater samples were used to evaluate the method's performance under real-world conditions and identify potential interferences. The samples were obtained from five localities in Hidalgo, a Central Mexican state extending north of Mexico City, and characterized in a previous work reported in 2020 [33]. Briefly, trace metals were determined in the rainwater according to the Environmental Protection Agency of the United States of America (EPA, USA) protocol, which employs a direct aspiration method by atomic absorption [34]. Total alkalinity and hardness were also determined using the Mexican standards NMX-

AA-036-SCFI-2001 [35] and NMX-AA-072-SCFI-2001 [36], respectively. Composite mixed samples resulted from the monthly accumulation of rainwater collected annually from the following sites: Tula (20.0522° N–99.3442° W), Pachuca (20.1011° N–98.7591° W), Tulancingo (20.0905° N–98.3691° W), Agua Blanca (20.3465° N–98.3595° W), and Molango (20.7908° N–98.7288° W) [33]. The rainwater samples were filtered (with Whatman filter No. 40) and stored in glass containers until their analysis by the SPR technique.

2.3. Measurement Procedure with Angular Interrogation

The plasmonic system consists of a homemade platform, previously described in detail by our research group in Refs. [37,38]. The angular interrogation scheme measures the reflected light from the SPR sensor during angular scans, i.e., by varying the angle of incidence of the laser light. At a specific angle, the incident light over the gold film excites the metal's conduction electrons, leading to a collective oscillation known as a surface plasmon [19]. This study employed p-polarized laser light of 633 nm (N-LHP, Newport Corp., Irvine, CA, USA) to generate the plasmon phenomena. During the angular interrogation measurements, the SPR angle, corresponding to the minimal reflectance intensity, is detected, and its displacement is related to changes in the optical properties of the dielectric medium (refractive index variations due to absorption events in the thin film). Thus, angular scans were performed for every microplastic solution at different concentrations to observe the relationship between the response and the concentration of various microplastics, as measured by the shift in the resonance angle. The solutions were flowed to the system by a syringe pump (Legato 100, KDScientific, Boston, MA, USA) at a rate of 30 μL min^{-1}, and three replicates of each solution were measured.

2.4. Laccase-Based SPR Setup

A Kretschmann configuration was employed for the setup, comprising two rotation plates and a stepper motor that allows for synchronized movement to obtain a θ–2θ system. Additionally, the platform features a Teflon cell that enables the continuous flow of solutions required during analysis, which come into contact with a gold-coated chip optically coupled to a prism (with an oil matching index of 1.51) [38]. The sensor chips fabrication comprised evaporating thin films of 3 nm chromium and 50 nm gold on the prism, employing a vacuum chamber (High Vacuum Coating Plant BA510, Balzers High Vacuum Corp., Santa Ana, CA, USA). Then, a gold film of 50 nm was deposited by thermal evaporation at a rate of 5 Å/s and 8×10^{-6} mbar.

Laccase immobilization on the plasmonic chip was performed according to the well-known coupling protocol, in which clean and dried gold chips were incubated by immersion in a solution of alkanethiols at 250 μM (MHDA: MUD dissolved in ethanol) for 12 h at room temperature. During this process, one of the functional groups of the alkanethiol chains binds to the gold surface by its sulfur group, leaving the terminal carboxylic group free on the terminal side of the chain for further activation [39]. The activation occurs by the formation of carbodiimide esters with the addition of EDC/NHS crosslinkers (0.2 M/0.05 M, respectively) dissolved in MES buffer at 100 mM, pH 5 [39]. After a washing step with water to remove excess reagent, an enzymatic solution (containing laccase at 200 U mg^{-1}) is added to facilitate enzyme immobilization through the formation of an amide bond. Once the attachment process is concluded, surface passivation is performed by adding ethanolamine at 1M, preventing unspecific bindings [39]. The prepared chip is washed with a PBS buffer solution and stored in the same buffer at 4 °C until its use (see Figure 1).
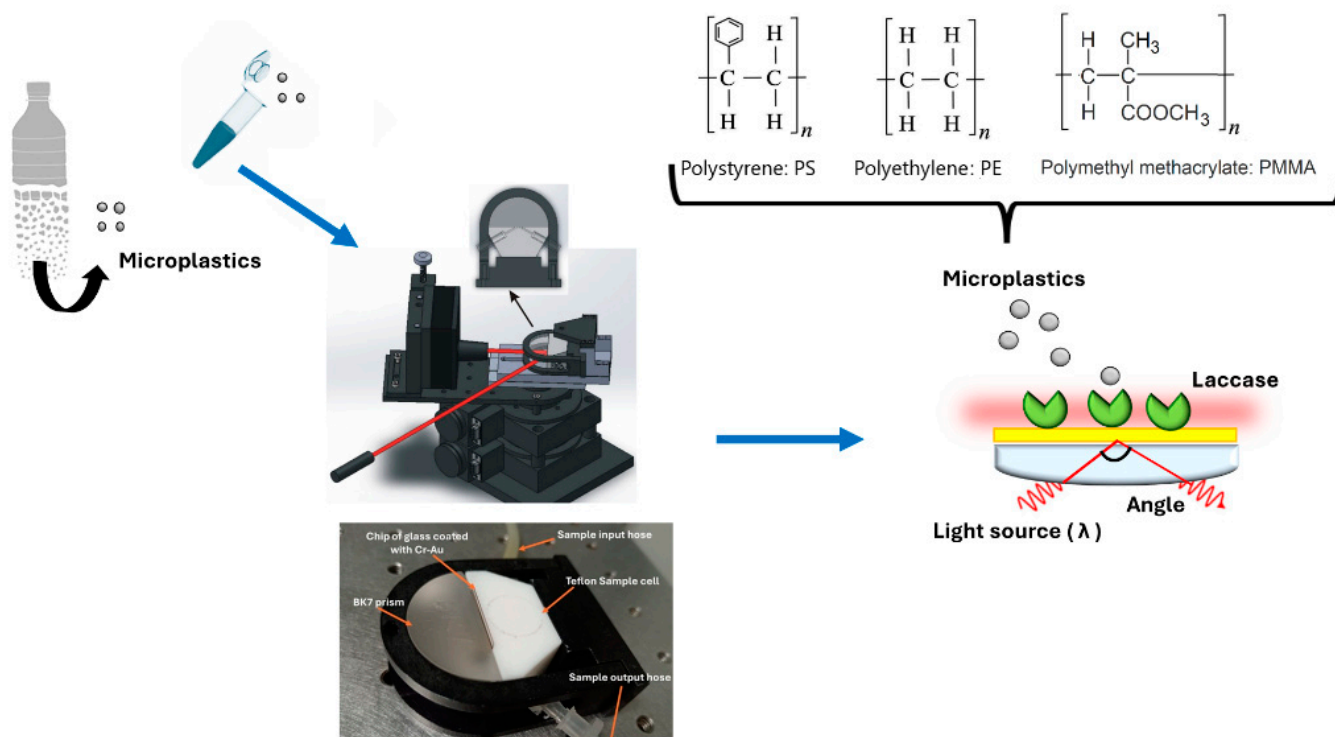
Figure 1. Schematic diagram of laccase-SPR biosensor.

2.5. SPR Measurements at a Fixed Angle

Measurements conducted under a fixed-angle scheme enable the monitoring of reflectance intensity over time while analyzing microplastic solutions. The fixed angle was established at the midpoint of the slope in the Surface Plasmon Resonance (SPR) curve, which corresponds to the region of highest sensitivity to changes in light intensity, which were monitored as a function of time during the measurement of the solutions [20]. The reflectance intensity in the assay was attributed to the interaction between the receptor and the target molecule. Once the chip immobilized with laccase was mounted on the SPR setup, a fluidic system flowed with PBS buffer at a rate of 30 μL/min, which served as the running solution during the measurement process. Microplastic samples at various concentrations were injected at the same rate over the sensor surface (See Figure 1). Through a direct enzyme/substrate assay, a shift in the refractive index is detected, which is measured by the photodetector due to the enzyme's conformational changes during the binding process (enzyme/substrate interaction between laccase and microplastics) [40]. Consequently, the signals obtained are directly proportional to the concentration of plastic particles in the sample.

Afterward, the sensor surface was washed with PBS buffer to remove weakly bound particles. This was followed by the injection of a regeneration solution of 10 mM NaOH for 20 s, preparing the system for the next measurement cycle. All measurements were performed in triplicate, and the average SPR signals were plotted against the concentration of microplastics in the sample. The calibration curve generated from this data was used to establish the biosensor's analytical parameters. The slope of this curve indicates the sensitivity of the method. The limit of detection (LOD) was evaluated as three times the baseline's standard deviation, while the limit of quantitation (LOQ) was set at ten times the standard deviation. Finally, spiked real samples were tested under the same SPR testing conditions to assess the recovery of the analytical procedure and evaluate potential matrix effects. Rainwater samples were spiked at one level of fortification with microplastic suspension at 4000 μg mL^{-1}. This process is designed to verify the sensor's effectiveness under conditions similar to those of the actual environment.

3. Results and Discussion

3.1. Measurement of Micro and Nano Plastic Working Solution with Angular Interrogation

Working solutions were prepared using commercial standard suspensions (10% *w/v*) of spherical particles made of polystyrene (PS, 0.1 μm diameter), polymethyl methacrylate (PMMA, 1.0 μm and 100 μm diameter), and polyethylene (PE, 34–50 μm diameter). The selection criteria for the polymeric particles focused on their environmental prevalence. As detailed in the review by Rossatto et al. (2023), the most commonly found microplastics (MPs) are polypropylene (PP, 16.05%), polyethylene (PE, 15.43%), polystyrene (PS, 10.49%), polyamide/nylon (PA, 7.41%), polyvinyl chloride (PVC, 6.79%), poly(methyl methacrylate/polyacrylate/acrylate/acrylic) (PMMA, 6.17%), and polyester (PES, 5.56%) [41]. The studies included in this review were gathered from the Science Direct database on three different dates in 2020, focusing on the occurrence of microplastics and revealing the types found across continents. Asia and Europe had a higher volume of research related to microplastic presence. Based on this, we selected PE particles as a model of MPs with high environmental occurrence, followed by PS, which appears with moderate frequency, and PMMA, which is less common. Additionally, the chosen particle sizes (ranging from 0.1 to 100 μm), covering both nanoplastics (under 1 μm) and microplastics (1–5 mm) scales, address current detection challenges in environmental monitoring [3–5]. These size ranges are also frequently reported in occurrence studies, especially between 100 and 5000 μm.

Once the working solution measurements (ranging from 0 to 6000 μg/mL) were obtained using an angular interrogation scheme on the SPR platform, angular scans were produced, showing shifts in the resonant angle for the different microplastic polymers. These scans also showed the relationship between the response and concentration of each plastic. The solutions were introduced to the system at a rate of 30 μL/min. Figure 2 displays scans of the solutions, all at the same concentration (600 μg/mL), revealing differences in resonance angles. This indicates a shift of approximately 0.1° as the particle size increases by one degree. For example, the 0.1 μm particle solution had a resonance angle of 71.4°, while the 100 μm solution had a resonance angle of 71.7°, indicating that as particle size increases, both the angular displacement and depth also increase. There is a direct relationship between the resonant angle of the SPR curve and the refractive index. As a result, any increase in this parameter causes the resonance notch to shift toward higher angles [42]. In this sense, the 100 μm solution exhibited the highest resonance angle (71.7°), suggesting that it possesses the highest refractive index among the tested solutions. Usually, at the resonance angle, the reflectance drops to nearly zero because the evanescent wave decays due to total internal reflection in the system [42]. As a result, when the sample is a non-absorbent medium, the SPR curve becomes narrower and deeper, with a sharp point which corresponds to the point of lowest reflectance (the minimum intensity value, R_{min}) [43]. From this perspective, the 0.1 μm particle solution had the highest R_{min} value, indicating the sample represents a strongly absorbing medium [44]. This happens because the absorption peak of these species coincides with the plasmonic resonance wavelength. As a result, the evanescent field is weakened, leading to plasmonic inhibition and a less steep SPR curve [42]. Both the width and depth of the SPR curve are influenced by the imaginary part of the refractive index, particularly the extinction coefficient [43].

For each particle size suspension (0.1, 1.0, 34–50, and 100 μm), working solutions were prepared by serially diluting them in a 90:10 water/phosphate buffer solution (by volume). The tested concentration of these working solutions ranged from 0 to 9000 μg/mL. When analyzing the solutions for 0.1 μm, no significant differences in angular shifts were observed among the tested concentrations (see Figure 3). This suggests a very similar refractive index, as indicated by the resonant angle, with only slight differences in the curve's width related to absorbent components. However, a higher-resolution system would

provide more information about the SPR curve parameters of the samples. Interestingly, the 1 μm particle solution showed a slight angular shift, rising from 71.56° to 71.64° as the concentration increased (from 300 to 6000 μg/mL). While this implies a rise in refractive index, it is also accompanied by a plasmon curve that changes in depth with higher concentration. This suggests a non-absorbing effect of the medium. Regarding the solutions of higher sizes, 34–50 and 100 μm, a noticeable angular shift toward higher angles was observed as the refractive index increased with concentration. In this sense, angular interrogation measurements reveal unique features in the SPR curve parameters for each size solution, making them a useful tool for characterizing and distinguishing between microplastics of different sizes. However, to enhance the resolution for accurate measurement of concentrations, we utilized laccase enzymes as a receptor in a second step to boost detection.
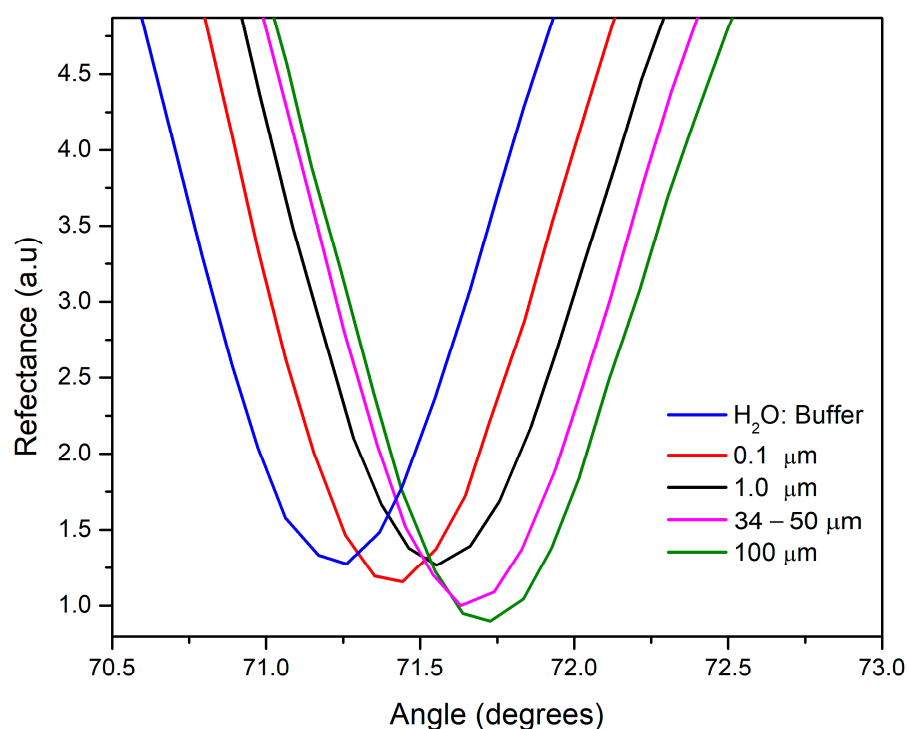

Figure 2. SPR curves at interrogation angle of four microplastic solutions (from 0.1 to 100 μm), using water/buffer mixture as reference for pointing the resonant angles displacements.

3.2. Measurement of Micro and Nanoplastic Working Solution at Fixed Angle

A laccase enzyme was used to interact with micro- and nanoplastics immobilized on a gold-coated chip that had been functionalized with alkanethiols and subsequently activated through EDC/NHS crosslinkers. The detection involved a direct enzyme–substrate assay performed between laccase and the plastic particles, with concentrations ranging from 0 to 6000 μg/mL. This was conducted using the SPR platform at a fixed angle, allowing the reaction to be monitored over time. Here, the laccase enzyme catalyzed the oxidation of specific groups on the polymer chains of microplastics, causing the breakdown of C-O and C-N linkages [31]. This reaction results in a conformational shift of the enzyme during the catalytic event, leading to a change in the refractive index (SPR signal) [40]. By analyzing the plastic particles and their impact on reflectance intensity, a positive correlation was observed between the concentration of the solutions and the response intensity (Figure 4).
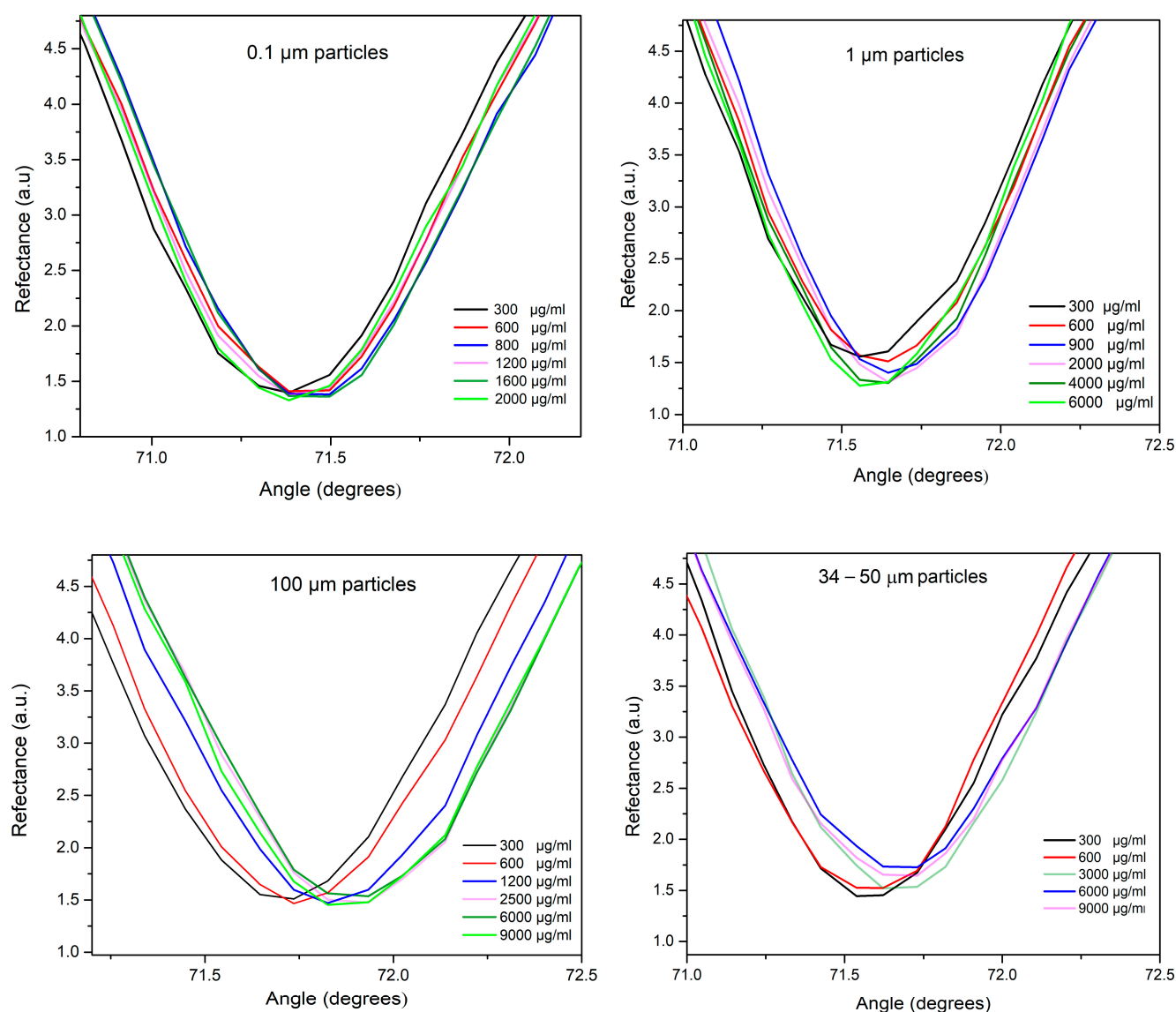
Figure 3. SPR curves at interrogation angle of each particle size suspension (0.1, 1.0, 34–50, and 100 μm) at different concentrations.

The analytical performance of the SPR-based biosensor developed for detecting micro- and nanoplastics demonstrated a clear dependence on both particle size and polymer type. As detailed in Table 1, the biosensor exhibited varying limits of detection (LOD), limits of quantification (LOQ), sensitivities, and dynamic ranges for different microplastic samples. For instance, particles of the same polymer (polymethylmethacrylate plastics) with sizes of 1 and 100 μm had LODs of 253.2 and 3.7 μg/mL, respectively. This indicates that the size of the plastic spheres influenced the analytical detection by the proposed biosensor, with lower detection occurring as the particle size decreased. In this sense, it has been reported that smaller particles have higher diffusion coefficients and surface-to-volume ratios, which increases the probability of encounters and the probability of adhering to surfaces, resulting in an adsorption effect of particles on the gold surface [45].
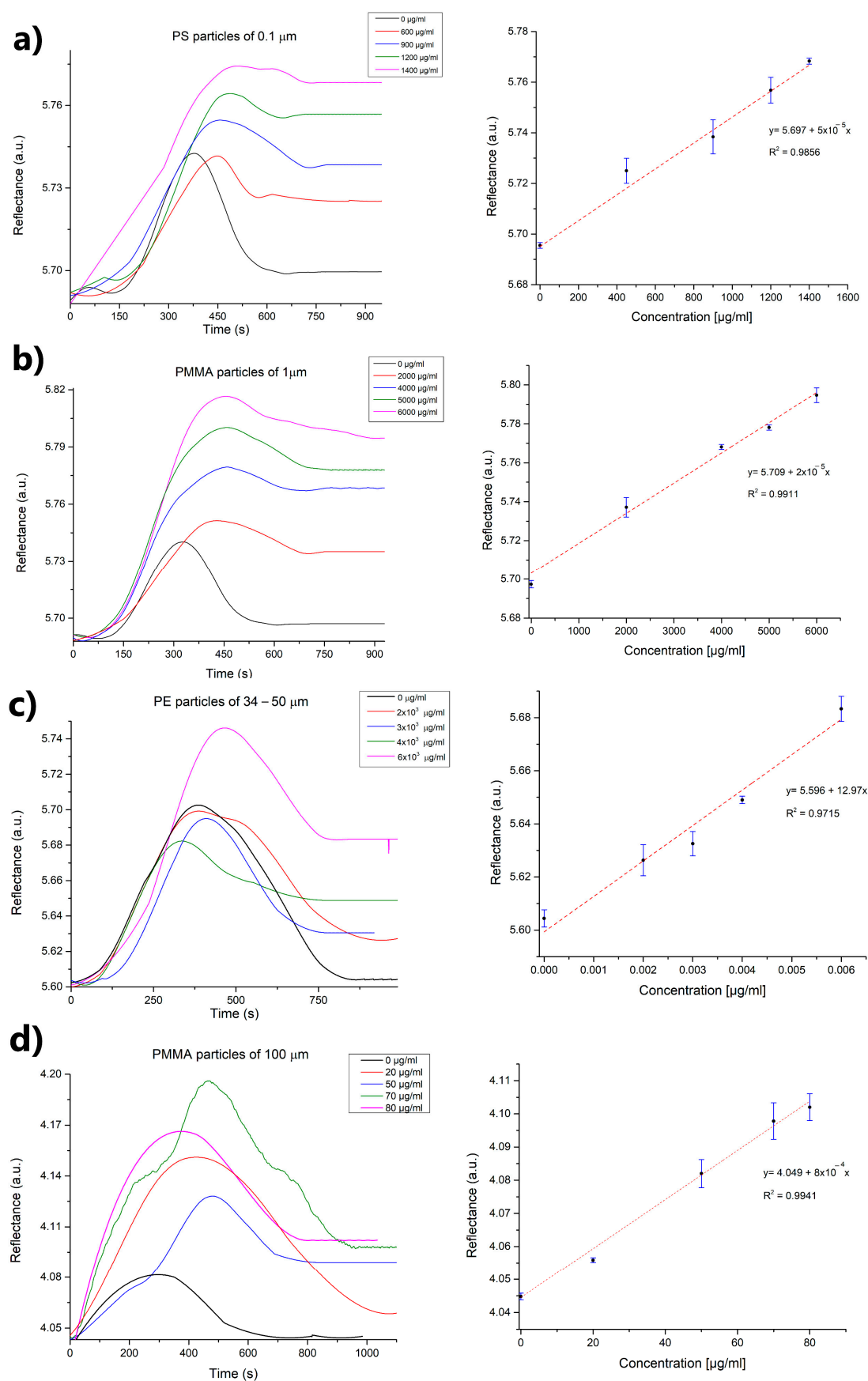
Figure 4. SPR sensorgrams of each particle size suspension ((**a**) 0.1, (**b**) 1.0, (**c**) 34–50, and (**d**) 100 μm) at different concentrations and calibration curves in water/PBS (*n* = 3).

Table 1. Analytical parameters of SPR-based biosensors micro- and nanoplastic detection.

Particle's Size	Limit of Detection (μg/mL)	Limit of Quantification (μg/mL)	Sensibility Reflectance/μg mL^{-1}	Dynamic Range (μg/mL)
Polystyrene particles 0.1 μm	68.3	227.5	4.9×10^{-5}	0–1400
Polymethylmethacrylate particles 1 μm	253.2	844.1	1.6×10^{-5}	0–6000
Polyethylene particles 35–50 μm	7.5×10^{-4}	2.5×10^{-3}	12.9	0–6000
Polymethylmethacrylate particles 100 μm	3.7	12.3	0.0008	0–80

According to Tuoriniemi et al. (2016), the SPR method was used to characterize polystyrene particles in colloidal suspensions at sizes ranging from 100 nm to 1000 nm [46]. The method measured the effective refractive index and compared the results to those predicted by coherent scattering theory (CST). The study found that for particles 100 nm in size (0.1 μm), the measured effective refractive index at low concentrations was higher than what CST predicted, attributed to the absorption on the gold surface [46]. Additionally was reported that as dispersions become more concentrated, the amplitude of the scattered light also decreases due to interference from light scattered by nearby particles [46]. Therefore, we hypothesize that particles may settle and prevent effective contact with the enzymes, thereby limiting binding reactions and producing a weak signal. However, further experiments are needed to confirm this possibility.

PS nanoparticles at 0.1 μm had a lower limit of detection (68.3 μg/mL) compared to PMMA microparticles at 1 μm (253.2 μg/mL), which contradicts reports suggesting that detection decreases as particle size reduces. This difference may be due to the enzyme's preference for PS over PMMA as a substrate, since laccases are versatile copper-containing oxidases with low substrate specificity. This allows them to act on a wide range of aromatic and non-aromatic compounds beyond their natural lignocellulosic substrates, although they show varying affinities toward them [30]. This catalytic flexibility has facilitated their application in the oxidative modification of synthetic polymers such as polyethylene [25], polyvinyl chloride [27], and polystyrene biodegradation [28,29]. Interestingly, polyethylene particles in the 35–50 μm range showed a lower LOD of 7.5×10^{-4} μg/mL (followed by the LOD of 3.7 μg/mL obtained for the 100 μm solution), indicating better detection performance for larger particles and a higher affinity of the laccase for the PE polymer. In this context, Santacruz-Juárez et al. reported that laccase from *Trametes versicolor* exhibited a binding affinity of 40.11 μM toward PE, outperforming other ligninolytic enzymes such as manganese peroxidase (82.16 μM) and lignin peroxidase (66.93 μM), and second only to unspecific peroxygenase (34.34 μM). These findings highlight the potential of laccase as a biocatalyst for plastic transformation or degradation under environmentally relevant conditions [47].

Lastly, the sensitivity of our biosensor, measured as reflectance per μg/mL, varied from 1.6×10^{-5} for PMMA (1 μm solutions) to 12.9 for PE (35–50 μm solutions), highlighting how both material properties and particle size impact the biosensor's response. The dynamic detection range was largest for particles of intermediate size, with PMMA (1 μm) and polyethylene (35–50 μm) covering a range of 0–6000 μg/mL. In contrast, the range was narrower for the smallest and largest particles tested, such as polystyrene (0.1 μm, 0–1400 μg/mL) and PMMA (100 μm, 0–80 μg/mL). For 0.1 μm particles, higher concentrations led to sedimentation and loss of solution homogeneity, while for 100 μm solutions, concentrations above 80 μg/mL produced no measurable SPR signals. Also, the immobilized enzyme retained its recognition capacity for up to 25 regeneration cycles using 10 mM NaOH, before a significant loss of signal was observed.

Setting a detection range relevant to environmental MPs concentrations is complicated because the presence of microplastics in aquatic environments is usually expressed in particles/m^3 or units/m^3. However, in laboratory settings, it is necessary to work with small, concentrated volumes, often reported as µg/mL or ng/mL depending on the sensitivity of the technology used. These measurements are obtained from large-volume samples recovered through 'reduced volume' sampling methods, which involve in situ filtration with trawl nets and pump-and-sieve samplers towed by boats. Therefore, we based the detection range for our study on a review of existing sensing and biosensing research (see Table 2). Comparing these results to those of earlier sensor technologies shows that the proposed SPR biosensor has similar detection performance for microplastic sizes between 10 and 20 µm. For instance, chronoamperometric detection using carbon electrodes achieved a limit of detection (LOD) as low as 5×10^{-4} µg/mL for 10 µm polystyrene particles. Similarly, an SPR-based platform combined with an estrogen receptor reached LODs of 3.9×10^{-4} µg/mL for 20 µm PMMA particles in seawater. However, for particles 1 µm in size, the method based on surface-enhanced Raman spectroscopy (SERS) yielded better LODs. These findings demonstrate that SPR can be a valuable tool for measuring microplastics. Nevertheless, a key consideration in using SPR-based particle detection is that particles often adhere to surfaces, emphasizing the need to optimize the current setup, especially to boost its sensitivity to nanoparticles.

Table 2. Performance summary of various sensors to detect microplastics.

Micro and Nanoplastics Detection				
Method	Analyte	Limit of Detection	Measurement Conditions	Reference
Plasmon-enhanced fluorescence (PEF)	Low-density polyethylene (LDPE), poly(butylene adipate-co-terephthalate) (PBAT) from 0.8 to 2.5 µm	Not reported	Gold nanopillar substrates Sample: miliQ water	[48]
Matrix-Assisted Laser Desorption/Ionization coupled to time-of-flight mass spectrometry (MALDI-TOF MS)	Not reported	25 µg/mL	Thermal pre-treatment	[49]
Pyrolysis Gas Chromatography-Mass Spectrometry (Pyro-GC/MS)	Not reported	4 µg/mL	Complex sample pre-treatment	[50]
Fourier Transform Infrared (FT-IR) Spectroscopy	50–500 µm	Not reported	Not reported	[51]
Surface Plasmon Resonance (SPR)	Poly(methyl methacrylate) nanoparticles of 20 and 0.1 µm	3.9×10^{-4} µg/mL	SPR platform with a polymer-based gold nanograting using an estrogen receptor (ER) as recognition element Sample: seawater	[22]
Localized surface plasmon resonance (LSPR) sandwich	Polystyrene 10 µm	1 µg/mL	Gold nanoparticles coupled to PS-targetedoligo-peptide Sample: Deionized water	[23]
Resistive pulse sensors	Microparticles 21.9 µm	6.52×10^{-4} particles/mL	Salt concentrations ranging from 2.5×10^{-4} to 0.1 M Sample: teabags	[52]
Chronoamperometry	Polystyrene 0.1 to 10 µm	5×10^{-6}–5×10^{-4} µg/mL	Carbon electrodes with ferrocene as mediator Sample: water	[53]
Surface-enhanced Raman spectroscopy (SERS)	Polystyrene 1 µm and 0.05 µm	40 µg/mL	Silver nanoparticles, Sample: seawater	[54]
	Polystyrene 1 µm	5 µg/mL	Silver nanoparticles, Sample: river water	[55]

3.3. Evaluation of SPR Performance with Rainwater Sample: Study of Matrix Effects

In addition to validation under controlled conditions (using PBS buffer), the biosensor's performance was tested using rainwater samples from Mexico's Molango and Tula regions. As shown in Table 3, these samples contain a range of metal ions and trace elements, which were a concern due to potential matrix effects. Some of these elements are known to interfere with enzymatic systems such as laccase. This is because they could

lead to false positives or non-specific bindings that hinder bioreceptor recognition [56]. Laccases are multicopper oxidases that rely on coordinated copper ions in their active sites for electron transfer. Thus, certain metal ions in environmental samples can disrupt this coordination, affecting their enzymatic activity [57,58].

Table 3. Significant ion concentrations (mg/L) in rainwater samples.

Analytical Parameters	Rainwater Sample		Mexican Permissible Limits [33]
	Molango	**Tula**	
pH	6.0	5.5	-
CO_3^{-2}	20	20	-
Fe	0.448	0.472	0.3
Mn	0.148	0.074	0.15
Cr	0.055	0.036	0.05
Cu	0.047	0.045	2
Ni	0.012	0.033	-
Co	0.013	0.015	-
Pb	0.031	0.028	0.025
Zn	0.282	0.137	5
Cd	0.001	0.002	0.005
As	0.002	0.004	0.005

Therefore, to assess potential matrix effects from rainwater composition, we analyzed samples spiked at a single fortification level (4000 µg/mL) with a microplastic suspension (1 µm) in triplicate under the same SPR testing conditions. Initially, no significant SPR signal was observed (non-specific binding) during preliminary analysis with only rainwater samples (see Figure 5). However, the SPR biosensor showed a significant under-recovery of 58% in samples from Molango, which contained high concentrations of Mn^{2+}, Cr^{2+}, and Zn^{2+}. In contrast, samples from Tula showed recovery rates of 113%. These ions may have interfered with laccase activity, since Ni^{2+}, Pb^{2+}, Zn^{2+}, and Mn^{2+}, which were detected in both rainwater samples, are known to inhibit laccase by binding to the enzyme's copper centers in a competitive or non-competitive manner [59]. Ni^{2+} has been shown to decrease laccase activity by affecting the redox potential and structural stability of the enzyme. Similarly, Pb^{2+} binds to carboxylate groups near the active site, impairing the enzyme's function [60]. Zn^{2+}, although not directly involved in redox reactions, can cause steric hindrance at substrate-binding sites, reducing enzyme affinity. Finally, Mn^{2+} can alter the enzyme's secondary structure and, in some cases, slightly inhibit its catalytic activity [61].

Although reduced laccase activity can result from changes in binding affinity or electron transfer efficiency caused by ion concentration, it is also important to consider the ions' role in destabilizing microplastic particles. This instability can cause aggregation, which affects interactions with the immobilized laccase enzyme and the sensor surface, thereby impacting the SPR signal. Microplastics generally have characteristic surface charges that depend on polymer type, size, pH, ionic strength, and environmental conditions. In this sense, studies show that PE, PS, and PMMA particles usually carry a moderately negative surface charge at neutral pH, typically between −15 mV and −50 mV [62,63]. However, the presence of divalent cations such as Ca^{2+}, Mg^{2+}, Mn^{2+}, Cr^{2+}, or Zn^{2+} (like those found in rainwater) neutralizes this negative charge, thereby decreasing the electric double layer thickness [64]. The reduction of the double layer lowers the energy barrier in the Lennard–Jones potential, and thereby facilitates aggregation via van der Waals and electrostatic forces after particle collisions [65]. At low ion concentrations, electrostatic repulsion stabilizes the dispersions, whereas at high concentrations, van der Waals attractions promote MP

aggregation. Notably, monovalent cations like Na^+ and K^+ result in fewer aggregates and do not affect zeta potential in MPs when Cl^-, HCO_3^-, and SO_4^{2-} are present [66].
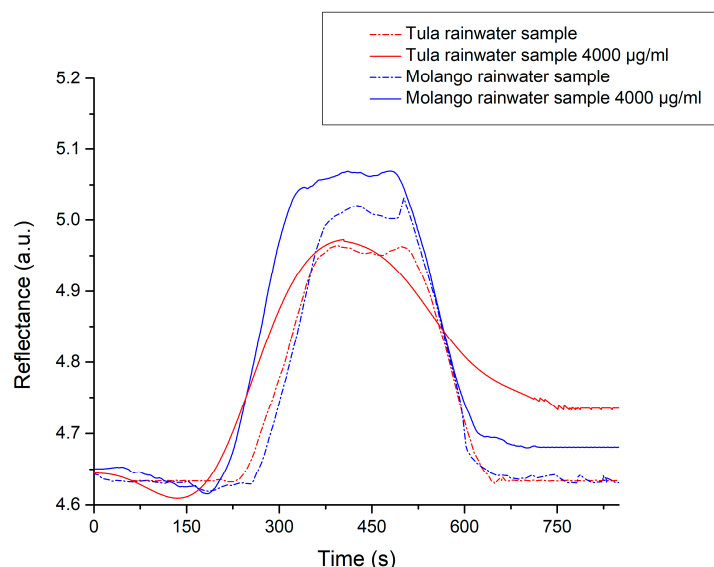

Figure 5. Evaluation of non-specific signals due to matrix effects from the rainwater (*n* = 3).

This work presents an initial approach to using laccase enzymes as recognition elements for detecting MPs. However, it does not address interference from non-plastic particles like silica, cellulose, clays, algae, or organic matter, which could be an additional limitation. Additionally, since laccase exhibits a high capacity for non-specific oxidation, further selectivity tests are needed to confirm its effectiveness in real-world environments. These environments may contain not only soil particles and plant debris but also other pollutants like quinol, resorcinol, catechol, phenol, 2,4-dichlorophenol, and humic acid [67]. These substances could be adsorbed onto MPs or act as plastic additives, including pigments, stabilizers, and flame retardants. Furthermore, environmental weathering of plastics further alters their physicochemical characteristics, promoting their oxidation, increasing their hydrophilicity, and altering their shape (fragments, pellets, fibers, flakes) [68]. Thus, all these surface modifications would diminish the SPR signal or inhibit it altogether.

4. Conclusions

In this study, we developed a proof-of-concept plasmonic biosensor for detecting microplastics and nanoplastics in rainwater samples. The Surface Plasmon Resonance (SPR) measurements conducted at a fixed angle allowed us to optically characterize different particle size suspensions (0.1, 1.0, 34–50, and 100 μm). Our results demonstrated well-differentiated characteristics based on SPR parameters. For instance, the solutions exhibited resonant angle displacements and an increased resonance depth as particle size increased. Specifically, the 0.1 μm particle solution had a resonance angle of 71.4°, while the 100 μm solution showed a resonance angle of 71.7°, indicating that both angular displacement and resonance depth increase with particle size. This study also explored the use of different biorecognition elements, utilizing laccase enzymes as receptors. This approach provided valuable information regarding the analytical performance of different receptors for the sensors. The laccase enzyme demonstrated good sensitivity, enabling the detection of various polymers and particle sizes without requiring sample pre-treatment. The lowest limit of detection was found for polyethylene (PE) particles at 35–50 μm (7.5×10^{-4} μg/mL), followed by polymethyl methacrylate (PMMA) at 100 μm (3.7 μg/mL), polystyrene (PS) at 1 μm (68.3 μg/mL), and PMMA at 0.1 μm (253.2 μg/mL). These results suggest that the

proposed biosensor could monitor microplastics in environmental samples without pretreatment. Although no significant matrix effects were observed in the SPR measurements of the rainwater samples, it is essential to perform selectivity assays to confirm the method's feasibility. This study demonstrates the potential of laccase-based SPR biosensors to improve microplastic detection and highlights the importance of considering matrix effects (interferences) for real applications. Such interferences may cause false positives or reduce the device's analytical accuracy because they are similar in size to plastic particles or trigger non-specific reactions. Future research could focus on microfluidic systems that separate MPs from interfering substances like algae, bacteria, proteins, and others that affect MP detection. Additionally, investigating other recognition elements, such as aptamers or enzymes that specifically target polymeric materials and resist environmental factors like pH and temperature, is crucial for enabling real-time field monitoring.

References

1. Mai, L.; Bao, L.; Shi, L.; Wong, C.S.; Zeng, E.Y. A review of methods for measuring microplastics in aquatic environments. *Environ. Sci. Pollut. Res.* **2018**, *25*, 11319–11332. [CrossRef]
2. Bui, X.T.; Vo, T.D.H.; Nguyen, P.T.; Nguyen, V.T.; Dao, T.S.; Nguyen, P.D. Microplastics pollution in wastewater: Characteristics, occurrence and removal technologies. *Environ. Technol. Innov.* **2020**, *19*, 101013. [CrossRef]
3. Ekvall, M.T.; Lundqvist, M.; Kelpsiene, E.; Šileikis, E.; Gunnarsson, S.B.; Cedervall, T. Nanoplastics formed during the mechanical breakdown of daily-use polystyrene products. *Nanoscale Adv.* **2019**, *1*, 1055–1061. [CrossRef]
4. *ISO/TR 21960*; Plastics-Environmental Aspects-State of Knowledge and Methodologies. International Organization for Standardization: Geneva, Switzerland, 2020. Available online: https://www.iso.org/standard/72300.html (accessed on 11 September 2024).
5. Kokalj, A.J.; Hartmann, N.B.; Drobne, D.; Potthoff, A.; Kühnel, D. Quality of nanoplastics and microplastics ecotoxicity studies: Refining quality criteria for nanomaterial studies. *J. Hazard. Mater.* **2021**, *415*, 125751. [CrossRef]
6. Rajmohan, K.V.S.; Ramya, C.; Viswanathan, M.R.; Varjani, S. Plastic pollutants: Effective waste management for pollution control and abatement. *Curr. Opin. Environ. Sci. Health* **2019**, *12*, 72–84. [CrossRef]
7. Liu, P.; Wu, X.; Liu, H.; Wang, H.; Lu, K.; Gao, S. Desorption of pharmaceuticals from pristine and aged polystyrene microplastics under simulated gastrointestinal conditions. *J. Hazard. Mater.* **2020**, *392*, 122346. [CrossRef]
8. Kedzierski, M.; Lechat, B.; Sire, O.; Le Maguer, G.; Le Tilly, V.; Bruzaud, S. Microplastic contamination of packaged meat: Occurrence and associated risks. *Food Packag. Shelf Life* **2020**, *24*, 100489. [CrossRef]
9. Yusuf, A.; Sodiq, A.; Giwa, A.; Eke, J.; Pikuda, O.; Eniola, J.O.; Ajiwokewu, B.; Sambudi, N.S.; Bilad, M.R. Updated review on microplastics in water, their occurrence, detection, measurement, environmental pollution, and the need for regulatory standards. *Environ. Pollut.* **2022**, *292*, 118421. [CrossRef]
10. Zhang, Z.; Chen, Y. Effects of microplastics on wastewater and sewage sludge treatment and their removal: A review. *Chem. Eng. J.* **2020**, *382*, 122955. [CrossRef]

11. Weisser, J.; Pohl, T.; Heinzinger, M.; Ivleva, N.P.; Hofmann, T.; Glas, K. The identification of microplastics based on vibrational spectroscopy data—A critical review of data analysis routines. *TrAC-Trends Anal. Chem.* **2022**, *148*, 116535. [CrossRef]

12. Schwaferts, C.; Niessner, R.; Elsner, M.; Ivleva, N.P. Methods for the analysis of submicrometer- and nanoplastic particles in the environment. *TrAC-Trends Anal. Chem.* **2019**, *112*, 52–65. [CrossRef]

13. Hendrickson, E.; Minor, E.C.; Schreiner, K. Microplastic Abundance and Composition in Western Lake Superior As Determined via Microscopy, Pyr-GC/MS, and FTIR. *Environ. Sci. Technol.* **2018**, *52*, 1787–1796. [CrossRef]

14. Fu, W.; Min, J.; Jiang, W.; Li, Y.; Zhang, W. Separation, characterization and identification of microplastics and nanoplastics in the environment. *Sci. Total Environ.* **2020**, *721*, 137561. [CrossRef] [PubMed]

15. Materić, D.; Kasper-Giebl, A.; Kau, D.; Anten, M.; Greilinger, M.; Ludewig, E.; van Sebille, E.; Röckmann, T.; Holzinger, R. Micro-and Nanoplastics in Alpine Snow: A New Method for Chemical Identification and (Semi)Quantification in the Nanogram Range. *Environ. Sci. Technol.* **2020**, *54*, 2353–2359. [CrossRef]

16. Singh, S.; Wang, J.; Cinti, S. Review—An Overview on Recent Progress in Screen-Printed Electroanalytical (Bio)Sensors. *ECS Sensors Plus* **2022**, *1*, 023401. [CrossRef]

17. Wang, S.; Xu, M.; Jin, B.; Wünsch, U.J.; Su, Y.; Zhang, Y. Electrochemical and microbiological response of exoelectrogenic biofilm to polyethylene microplastics in water. *Water Res.* **2022**, *211*, 118046. [CrossRef]

18. Gongi, W.; Touzi, H.; Sadly, I.; Ben Ouada, H.; Tamarin, O.; Ben Ouada, H. A Novel Impedimetric Sensor Based on Cyanobacterial Extracellular Polymeric Substances for Microplastics Detection. *J. Polym. Environ.* **2022**, *30*, 4738–4748. [CrossRef] [PubMed]

19. Mayer, K.M.; Hafner, J.H. Localized Surface Plasmon Resonance Sensors. *Chem. Rev.* **2011**, *111*, 3828–3857. [CrossRef] [PubMed]

20. Estevez, M.-C.; Otte, M.A.; Sepulveda, B.; Lechuga, L.M. Trends and challenges of refractometric nanoplasmonic biosensors: A review. *Anal. Chim. Acta* **2014**, *806*, 55–73. [CrossRef]

21. Huang, C.J.; Narasimha, G.V.; Chen, Y.C.; Chen, J.K.; Dong, G.C. Measurement of Low Concentration of Micro-Plastics by Detection of Bioaffinity-Induced Particle Retention Using Surface Plasmon Resonance Biosensors. *Biosensors* **2021**, *11*, 219. [CrossRef]

22. Seggio, M.; Arcadio, F.; Cennamo, N.; Zeni, L.; Bossi, A.M. A plasmonic gold nano-surface functionalized with the estrogen receptor for fast and highly sensitive detection of nanoplastics. *Talanta* **2024**, *267*, 125211. [CrossRef]

23. Oh, S.; Hur, H.; Kim, Y.; Shin, S.; Woo, H.; Choi, J.; Lee, H.H. Peptide specific nanoplastic detection based on sandwich typed localized surface plasmon resonance. *Nanomaterials* **2021**, *11*, 2887. [CrossRef] [PubMed]

24. Santo, M.; Weitsman, R.; Sivan, A. The role of the copper-binding enzyme–laccase–in the biodegradation of polyethylene by the actinomycete Rhodococcus ruber. *Int. Biodeterior. Biodegradation* **2013**, *84*, 204–210. [CrossRef]

25. Sowmya, H.V.; Krishnappa, M.; Thippeswamy, B. Degradation of polyethylene by Trichoderma harzianum—SEM, FTIR, and NMR analyses. *Environ. Monit. Assess.* **2014**, *186*, 6577–6586. [CrossRef] [PubMed]

26. Albertsson, A.C.; Andersson, S.O.; Karlsson, S. The mechanism of biodegradation of polyethylene. *Polym. Degrad. Stab.* **1987**, *18*, 73–87. [CrossRef]

27. Chaudhary, A.K.; Vijayakumar, R.P. Studies on biological degradation of polystyrene by pure fungal cultures. *Environ. Dev. Sustain.* **2020**, *22*, 4495–4508. [CrossRef]

28. Hou, L.; Majumder, E.L. Potential for and distribution of enzymatic biodegradation of polystyrene by environmental microorganisms. *Materials* **2021**, *14*, 503. [CrossRef]

29. Milstein, O.; Gersonde, R.; Huttermann, A.; Chen, M.J.; Meister, J.J. Fungal biodegradation of lignopolystyrene graft copolymers. *Appl. Environ. Microbiol.* **1992**, *50*, 3225–3232. [CrossRef]

30. Arregui, L.; Ayala, M.; Gómez-Gil, X.; Gutiérrez-Soto, G.; Hernández-Luna, C.E.; de los Santos, M.H.; Levin, L.; Rojo-Domínguez, A.; Romero-Martínez, D.; Saparrat, M.C.; et al. Laccases: Structure, function, and potential application in water bioremediation. *Microb. Cell Fact.* **2019**, *18*, 200. [CrossRef]

31. Temporiti, M.E.E.; Nicola, L.; Nielsen, E.; Tosi, S. Fungal enzymes involved in plastics biodegradation. *Microorganisms* **2022**, *10*, 1180. [CrossRef]

32. Anand, U.; Dey, S.; Bontempi, E.; Ducoli, S.; Vethaak, A.D.; Dey, A.; Federici, S. Biotechnological methods to remove microplastics: A review. *Environ. Chem. Lett.* **2023**, *21*, 1787–1810.

33. Rivera-Rivera, D.M.; Escobedo-Urías, D.C.; Jonathan, M.P.; Sujitha, S.B.; Chidambaram, S. Evidence of natural and anthropogenic impacts on rainwater trace metal geochemistry in central Mexico: A statistical approach. *Water* **2020**, *12*, 192. [CrossRef]

34. United States of America, Environmental Protection Agency. Test Method 7000B: Flame Atomic Absorption Spectrophotometry, rev.02. Hazardous Waste Test Methods-SW-846. 2007. Available online: https://www.epa.gov/hw-sw846/sw-846-test-method-7000b-flame-atomic-absorption-spectrophotometry (accessed on 11 September 2024).

35. *NMX-AA-036-SCFI-2001*; Water Analysis-Determination of Acidity and Total Alkalinity in Natural Water, Wastewaters and Treated Wastewaters. Ministry of Economy of Mexico, Diario Oficial de la Federacion: Mexico City, Mexico, 2021. Available online: https://www.gob.mx/cms/uploads/attachment/file/166776/NMX-AA-036-SCFI-2001.pdf (accessed on 22 January 2024).

36. *NMX-AA-072-SCFI-2001*; Water Analysis—Determination of Total Hardness in Natural Water, Wastewaters and Treated Wastewaters. Ministry of Economy of Mexico, Diario Oficial de la Federacion: Mexico City, Mexico, 2001. Available online: https://www.gob.mx/cms/uploads/attachment/file/166788/NMX-AA-072-SCFI-2001.pdf (accessed on 22 January 2024).

37. Sánchez-Alvarez, A.; Luna-Moreno, D.; Hernández-Morales, J.A.; Zaragoza-Zambrano, J.O.; Castillo-Guerrero, G.H. Control of Stepper Motor Rotary Stages applied to optical sensing technique using LabView. *Opt.-Int. J. Light. Electron. Opt.* **2018**, *164*, 65–71. [CrossRef]

38. Luna-Moreno, D.; Sánchez-Álvarez, A.; Islas-Flores, I.; Canto-Canche, B.; Carrillo-Pech, M.; Villarreal-Chiu, J.F.; Rodríguez-Delgado, M. Early detection of the fungal banana black sigatoka pathogen Pseudocercospora fijiensis by an SPR immunosensor method. *Sensors* **2019**, *19*, 465. [CrossRef] [PubMed]

39. Soler, M.; Estevez, M.-C.; Alvarez, M.; Otte, M.A.; Sepulveda, B.; Lechuga, L.M. Direct detection of protein biomarkers in human fluids using site-specific antibody immobilization strategies. *Sensors* **2014**, *14*, 2239–2258. [CrossRef]

40. Sota, H.; Hasegawa, Y.; Iwakura, M. Detection of conformational changes in an immobilized protein using surface plasmon resonance. *Anal. Chem.* **1998**, *70*, 2019–2024.

41. Rossatto, A.; Arlindo, M.Z.F.; de Morais, M.S.; de Souza, T.D.; Ogrodowski, C.S. Microplastics in aquatic systems: A review of occurrence, monitoring and potential environmental risks. *Environ. Adv.* **2023**, *13*, 100396. [CrossRef]

42. Ekgasit, A.; Tangcharoenbumrungsuk, S.; Yu, F.; Baba, A.; Knoll, W. Resonance shifts in SPR curves of nonabsorbing, weakly absorbing, and strongly absorbing dielectrics. *Sens. Actuators B Chem.* **2005**, *105*, 532–541. [CrossRef]

43. Luna-Moreno, D.; Monzón-Hernández, D.; Noé-Arias, E.; Regalado, L.E. Determination of quality and adulteration of tequila through the use of surface plasmon resonance. *Appl. Opt.* **2012**, *51*, 5161–5167. [CrossRef]

44. Leite, I.; Navarrete, M.C.; Díaz-Herrera, N.; González-Cano, A.; Esteban, Ó. Selectivity of SPR fiber sensors in absorptive media: An experimental evaluation. *Sens. Actuators B Chem.* **2011**, *160*, 592–597. [CrossRef]

45. Bo, M.R.; Van der Zeeuw, E.A.; Koper, G.J.M. Kinetics of Particle Adsorption in Stagnation Point Flow Studied by Optical Reflectometry. *J. Colloid. Interface Sci.* **1998**, *197*, 242–250.

46. Tuoriniemi, J.; Moreira, B.; Safina, G. Determining number concentrations and diameters of polystyrene particles by measuring the effective refractive index of colloids using surface plasmon resonance. *Langmuir* **2016**, *32*, 10632–10640. [CrossRef] [PubMed]

47. Santacruz-Juárez, E.; Buendia-Corona, R.E.; Ramírez, C.; Sánchez, R.E. Fungal enzymes for the degradation of polyethylene: Molecular docking simulation and biodegradation pathway proposal. *J. Hazard. Mater.* **2021**, *411*, 125118. [CrossRef] [PubMed]

48. Wei, X.F.; Bohlén, M.; Lindblad, C.; Hedenqvist, M.; Hakonen, A. Microplastics Generated from a Biodegradable Plastic in Freshwater and Seawater. *Water Res.* **2021**, *198*, 117123. [CrossRef]

49. Mintenig, S.M.; Bäuerlein, P.S.; Koelmans, A.A.; Dekker, S.C.; Van Wezel, A.P. Closing the Gap between Small and Smaller: Towards a Framework to Analyse Nano- and Microplastics in Aqueous Environmental Samples. *Environ. Sci. Nano* **2018**, *5*, 1640–1649. [CrossRef]

50. Lin, Y.; Huang, X.; Liu, Q.; Lin, Z.; Jiang, G. Thermal Fragmentation Enhanced Identification and Quantification of Polystyrene Micro/Nanoplastics in Complex Media. *Talanta* **2020**, *208*, 120478. [CrossRef]

51. Xie, L.; Gong, K.; Liu, Y.; Zhang, L. Strategies and Challenges of Identifying Nanoplastics in Environment by Surface-Enhanced Raman Spectroscopy. *Environ. Sci. Technol.* **2023**, *57*, 25–43. [CrossRef]

52. Pollard, M.; Hunsicker, E.; Platt, M. A tunable three-dimensional printed microfluidic resistive pulse sensor for the characterization of algae and microplastics. *ACS Sens.* **2020**, *5*, 2578–2586. [CrossRef]

53. Vidal, J.C.; Midón, J.; Vidal, A.B.; Ciomaga, C.; Laborda, F. Detection, quantification, and characterization of polystyrene microplastics and adsorbed bisphenol A contaminant using electroanalytical techniques. *Microchim. Acta* **2023**, *190*, 203. [CrossRef]

54. Lv, L.; He, L.; Jiang, S.; Chen, J.; Zhou, C.; Qu, J.; Lu, Y.; Hong, P.; Sun, S.; Li, C. In Situ Surface-Enhanced Raman Spectroscopy for Detecting Microplastics and Nanoplastics in Aquatic Environments. *Sci. Total Environ.* **2020**, *728*, 138449. [CrossRef]

55. Zhou, X.X.; Liu, R.; Hao, L.T.; Liu, J.F. Identification of Polystyrene Nanoplastics Using Surface Enhanced Raman Spectroscopy. *Talanta* **2021**, *221*, 121552. [CrossRef]

56. Estevez, M.-C.; Belenguer, J.; Gomez-Montes, S.; Miralles, J.; Escuela, A.M.; Montoya, A.; Lechuga, L.M. Indirect competitive immunoassay for the detection of fungicide Thiabendazole in whole orange samples by Surface Plasmon Resonance. *Analyst* **2012**, *137*, 5659–5665. [CrossRef]

57. Pardo, I.; Rodríguez-Escribano, D.; Aza, P.; de Salas, F.; Martínez, A.; Camarero, S. A highly stable laccase obtained by swapping the second cupredoxin domain. *Sci. Rep.* **2018**, *8*, 15669. [CrossRef] [PubMed]

58. Muthukumarasamy, N.; Jackson, B.; Joseph-Raj, A.; Sevanan, M. Production of Extracellular Laccase from Bacillus subtilis MTCC 2414 Using Agroresidues as a Potential Substrate. *Biochem. Res. Int.* **2015**, *2015*, 765190. [CrossRef] [PubMed]

59. Lorenzo, M.; Moldes, D.; Sanromán, M.Á. Effect of heavy metals on the production of several laccase isoenzymes by Trametes versicolor and on their ability to decolourise dyes. *Chemosphere* **2006**, *63*, 912–917. [CrossRef]

60. Enayatizamir, N.; Liu, J.; Wang, L.; Lin, X.; Fu, P. Coupling laccase production from Trametes pubescence with heavy metal removal for economic waste water treatment. *J. Water Process Eng.* **2020**, *37*, 101357. [CrossRef]

61. Lorenzo, M.; Moldes, D.; Couto, S.R.; Sanrómán, M.A. Inhibition of laccase activity from Trametes versicolor by heavy metals and organic compounds. *Chemosphere* **2005**, *60*, 1124–1128. [CrossRef]

62. Khademi, M.; Wang, W.; Reitinger, W.; Barz, D.P. Zeta potential of poly (methyl methacrylate)(PMMA) in contact with aqueous electrolyte–surfactant solutions. *Langmuir* **2017**, *33*, 10473–10482. [CrossRef]

63. Zhou, G.; Wang, Q.; Li, J.; Li, Q.; Xu, H.; Ye, Q.; Wang, Y.; Shu, S.; Zhang, J. Removal of polystyrene and polyethylene microplastics using PAC and FeCl3 coagulation: Performance and mechanism. *Sci. Total Environ.* **2021**, *752*, 141837. [CrossRef]

64. Li, S.; Liu, H.; Gao, R.; Abdurahman, A.; Dai, J.; Zeng, F. Aggregation kinetics of microplastics in aquatic environment: Complex roles of electrolytes, pH, and natural organic matter. *Environ. Pollut.* **2018**, *237*, 126–132. [CrossRef]

65. Rasteiro, M.G.; Koponen, A. Monitoring aggregation processes in multiphase systems: A review. *Powders* **2024**, *3*, 77–110. [CrossRef]

66. Lu, S.; Zhu, K.; Song, W.; Song, G.; Chen, D.; Hayat, T.; Alharbi, N.S.; Chen, C.; Sun, Y. Impact of water chemistry on surface charge and aggregation of polystyrene microspheres suspensions. *Sci. Total Environ.* **2018**, *630*, 951–959. [CrossRef] [PubMed]

67. Tanaka, K.; Takahashi, Y.; Kajiwara, T.; Matsukami, H.; Kuramochi, H.; Osako, M.; Suzuki, G. Identification and quantification of additive-derived chemicals in beached micro–mesoplastics and macroplastics. *Mar. Pollut. Bull.* **2023**, *186*, 114438. [CrossRef] [PubMed]

68. Sharma, S.; Basu, S.; Shetti, N.P.; Nadagouda, M.N.; Aminabhavi, T.M. Microplastics in the Environment: Occurrence, Perils and Eradication. *Chem. Eng. J.* **2021**, *408*, 127317. [CrossRef]